

Solubility Advantage of Amorphous Pharmaceuticals: II. Application of Quantitative Thermodynamic Relationships for Prediction of Solubility Enhancement in Structurally Diverse Insoluble Pharmaceuticals

Sharad B. Murdande · Michael J. Pikal · Ravi M. Shanker · Robin H. Bogner

Received: 29 March 2010 / Accepted: 30 August 2010 / Published online: 22 September 2010
© Springer Science+Business Media, LLC 2010

ABSTRACT

Purpose To quantitatively assess the solubility advantage of amorphous forms of nine insoluble drugs with a wide range of physico-chemical properties utilizing a previously reported thermodynamic approach.

Methods Thermal properties of amorphous and crystalline forms of drugs were measured using modulated differential calorimetry. Equilibrium moisture sorption uptake by amorphous drugs was measured by a gravimetric moisture sorption analyzer, and ionization constants were determined from the pH-solubility profiles. Solubilities of crystalline and amorphous forms of drugs were measured in de-ionized water at 25°C. Polarized microscopy was used to provide qualitative information about the crystallization of amorphous drug in solution during solubility measurement.

Result For three out of the nine compounds, the estimated solubility based on thermodynamic considerations was within two-fold of the experimental measurement. For one compound, estimated solubility enhancement was lower than experimental value, likely due to extensive ionization in solution and hence its sensitivity to error in pKa measurement. For the remaining five compounds, estimated solubility was about 4- to 53-fold higher than experimental results. In all cases where the theoretical solubility estimates were signifi-

cantly higher, it was observed that the amorphous drug crystallized rapidly during the experimental determination of solubility, thus preventing an accurate experimental assessment of solubility advantage.

Conclusion It has been demonstrated that the theoretical approach does provide an accurate estimate of the maximum solubility enhancement by an amorphous drug relative to its crystalline form for structurally diverse insoluble drugs when recrystallization during dissolution is minimal.

KEY WORDS amorphous · crystal · dissolution · re-crystallization · solubility · solubility enhancement · solute activity in amorphous · thermodynamics

INTRODUCTION

The enthalpy, entropy, and free energy of amorphous solids are high relative to the corresponding crystalline solid (1–4), and this higher free energy results in enhanced solubility and dissolution rates. Therefore, there is growing interest in utilizing the amorphous form to enhance oral bioavailability of poorly water-soluble drugs (5–8), but, historically, the accurate assessment of this solubility advantage has proven difficult (9–11).

Recently, we reported the development of a detailed thermodynamic approach to quantitatively determine the solubility advantage of an amorphous pharmaceutical relative to its crystalline counterpart (1). This approach is based on (a) evaluating the difference in free energy between amorphous and crystalline forms of a drug using differential scanning calorimetry (DSC) data, (b) quantifying the change in thermodynamic activity of the amorphous form due to absorption of water, and (c) quantifying the impact of degree of ionization on solubility of the two solid

S. B. Murdande · M. J. Pikal · R. H. Bogner
Department of Pharmaceutical Sciences, University of Connecticut
Storrs, Connecticut 06269, USA

M. J. Pikal · R. H. Bogner (✉)
Institute of Material Science, University of Connecticut
Storrs, Connecticut 06269, USA
e-mail: robin.bogner@uconn.edu

S. B. Murdande · R. M. Shanker
Pfizer Global R&D, Groton Labs
Groton, Connecticut 06340, USA

forms of the drug. Utilizing this approach, the theoretically determined solubility enhancement ratio for indomethacin, where re-crystallization during experimental determination of its solubility was minimal, has been shown to be in close agreement (1) with the experimental value; this prediction was much more accurate than that given in an earlier report (9). This new method does require the use of a limited number of experimental parameters (i.e., melting temperature and heat of fusion of the crystalline form, glass transition temperature of the amorphous form, heat capacity difference between crystal and amorphous forms, activity of hydrated amorphous solute, and ionization constant in the case of ionizable compounds) in order to calculate the theoretical solubility advantage of amorphous drugs, but the required measurements are routine in most industrial laboratories. The quantitative results of the thermodynamic analysis (1) may be summarized by the equation

$$R_s = \frac{(1 - \bar{\alpha}^c)}{(1 - \bar{\alpha}^a)} \cdot \exp[-I(a_2)] \cdot \exp\left[\frac{(\mu_2^{*a} - \mu_2^{*c})}{RT}\right] \quad (1)$$

where R_s is solubility enhancement ratio of the amorphous and crystalline forms.

The first term in Eq. 1, $\frac{(1 - \bar{\alpha}^c)}{(1 - \bar{\alpha}^a)}$ takes into account the differences in the ionization of amorphous and crystalline solute; $\bar{\alpha}^c$ is the fraction ionized for the crystalline solute at its solubility, $\bar{\alpha}^a$ is the fraction ionized for the amorphous solute at its solubility, and bars above the symbols refer to the ionization terms at equilibrium. At equilibrium, the fraction of ionized solute in solution is lower for the amorphous form because the fraction ionized decreases with increasing solution concentration. Note that “equilibrium” in this context refers to the equilibrium between solid and its saturated solution, which is often not attainable experimentally for amorphous solids due to intervention of re-crystallization. It should be emphasized that while the ionization term can be much less than unity for dissolution in pure water, for applications involving dissolution in a buffer system, such as the usual *in vivo* system, the ionization term is unity and does not impact the solubility enhancement ratio. The second term, $\exp[-I(a_2)]$, is the activity of the amorphous solute obtained by applying the Gibbs-Duhem equation to water sorption isotherm data for the amorphous solid, and the third term, $\left[\frac{(\mu_2^{*a} - \mu_2^{*c})}{RT}\right]$, is the impact of the change in standard-state chemical potential on transforming from the crystal to the dry amorphous state, as obtained from DSC measurements on amorphous and crystalline solids. R is the gas constant, and T is temperature at which measurement of solubility enhancement is desired. The derivation of Eq. 1 has been described earlier (1). The magnitude of each

of these three effects in the thermodynamic estimation of solubility advantage of amorphous solid is specific for each compound. For example, the first term reflects the impact of different degrees of ionization arising from the different solubilities of amorphous and crystalline forms to the solubility enhancement ratio. This term is unity for non-ionizable drugs and when solubility is measured in buffered solutions.

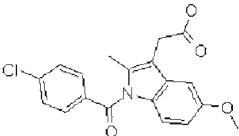
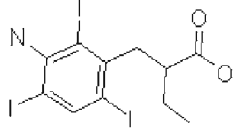
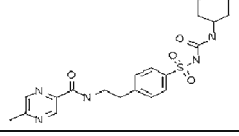
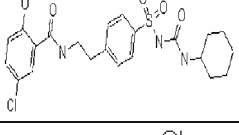
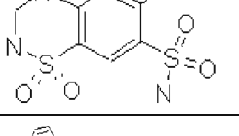
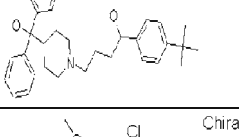
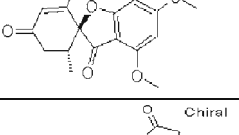
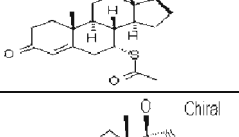
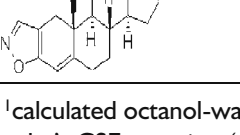
Utilizing this thermodynamic approach, we report here an assessment of the solubility advantage of amorphous forms of nine poorly soluble and structurally diverse drugs with a wide range of physico-chemical properties. This report compares the theoretically calculated solubility enhancement ratio, R_s , with the experimental measurements. The data also provide insights into the cause of observed differences between prediction and experimental results. Results from these investigations demonstrate that this thermodynamic approach may be routinely utilized by a formulator to quantitatively assess the advantage of utilizing an amorphous form or stabilized amorphous form as a drug delivery option for the potential enhancement of oral bioavailability of poorly water-soluble compounds.

Selection of Model Compounds

Model compounds for this research were selected based on intrinsic properties of drug molecules that are expected to contribute towards their insolubility in water. Insolubility of pharmaceuticals results primarily from high melting point (T_m , representing lattice energy) and/or high logP (lipophilicity). Semi-empirical quantitative methods developed by Yalkowsky (12–16) and Amidon (17) to estimate the solubility of crystalline organic solute use melting point and octanol-water partition coefficient (K_{ow} or P) as key descriptors linking solid-state and molecular properties to their aqueous solubility.

A compilation of the physicochemical properties of over 150 drugs from the WHO Model Lists of Essential Drugs (18) was used to select model compounds for this study. Salt forms of compounds were excluded from selection of compounds because salts are generally soluble and do not require additional solubility enhancement to provide acceptable bioavailability. Only unionized solid states of ionizable compounds (e.g. acid, base, and non-ionizable) were included as model compounds. While one cannot quantitatively predict solubility from T_m and/or logP, high T_m and high logP are generally associated with insolubility; hence, the pharmaceutical compounds selected have either relatively high octanol-water partition coefficient, i.e. logP > 3.5, relatively high melting point (>150°C), or both (Table I).

Table 1 Molecular Properties of Compounds Investigated in this Study

Drug	Structure	Mol. Wt. (Daltons)	clogP ¹	MP (°C) ²	Ionization	pKa ²	Solubility (µg/ml) ³	Solubility (µg/ml) ²
Indomethacin [#]		357.8	3.10	162.0	Acid	4.0	38.3	5.3
Iopanoic acid		570.9	4.19	152.3	Acid	4.4	6.2	14.4
Glipizide		445.5	2.07	198.3	Acid	4.9	221.7	4.1
Glybenclamide		494.0	3.75	173.7	Acid	5.5	9.0	0.2
Hydrochlorothiazide		297.7	-0.07	266.2	Acid (negligible ionization)	8.7, 10.4	4303.1	551.0
Terfenadine		471.7	6.51	150.0	Base	4.5	0.03	10.2
Griseofulvin	 Chiral	352.8	2.36	221.0	Non-ionizable	NA	53.4	8.6
Spirolactone	 Chiral	416.6	3.12	207.2	Non-ionizable	NA	15.1	30.0
Danazol	 Chiral	337.5	4.70	226.8	Non-ionizable	NA	0.2	0.3

NA, not applicable; ¹calculated octanol-water partition coefficient (ACD Labs); ²experimentally measured in this work; ³predicted by Yalkowsky's GSE equation (ref. 14); [#]data reported in ref. 1

All of the selected model compounds except terfenadine and iopanoic acid are compliant with Lipinski's "Rule of 5" criteria (19,20). Thus, all are at least nominally good candidates for drug products. Despite a narrow range of distribution of molecular weight among these model com-

pounds, the molecules represent diversity of chemical structure in terms of (a) fused *versus* isolated ring systems, (b) types of heterocyclic nuclei, (c) functional groups attached to ring systems, (d) chirality, (e) number of rotatable bonds, and (f) number of H-bond donors and acceptors in the molecule.

MATERIALS AND METHODS

Preparation of Amorphous Materials

Crystalline compounds indomethacin, iopanoic acid, terfenadine, glipizide, glybenclamide, griseofulvin, hydrochlorothiazide, spironolactone and danazol were purchased from Sigma Chemical Company (St. Louis, MO) and used as received. The crystallinity was confirmed by powder x-ray diffraction (PXRD), polarized light microscopy and DSC measurements. In addition, the moisture sorption of crystalline samples at expected monolayer ($\approx 35\%$ relative humidity) is $<0.01\%$, which is less than or equal to the expected monolayer coverage of a low specific surface area 100% crystalline sample, and is also $<0.1\%$ of the moisture sorption for the corresponding amorphous sample at 35% relative humidity. Thus, the amorphous contamination is less than 0.1%. The amorphous form of each of the model compounds was prepared by melting the crystalline form; the melt was kept at the temperature of melting for 5 min when it was obvious 100% molten material was obtained (by visual observation). The molten material was then quench-cooled by immersion into liquid nitrogen and ground in liquid nitrogen in a previously cooled mortar and pestle in a dry box to avoid condensation by moisture. The resulting melt-quenched samples were confirmed to be amorphous by the absence of birefringence under cross polarizers by optical microscopy, absence of a crystalline diffraction pattern by powder x-ray diffraction, and presence of glass transition (T_g) by differential scanning calorimetry (1). All amorphous samples were analyzed by reverse phase HPLC (high-performance liquid chromatography) as described in the HPLC analysis section to assess their chemical purity after melting and quench cooling. All amorphous compounds were determined to have $>99.9\%$ purity relative to the original crystalline sample. Amorphous samples were stored at -20°C over phosphorus pentoxide desiccant until use, and the water content of each of these samples was found to be below 0.2% w/w by Karl-Fisher titration.

Measurement of Thermal Properties, Ionization Constant and Moisture Sorption Isotherms for Use in Eq. 1

The procedures used to obtain the values required in Eq. 1 were previously described (1). Briefly, the following measurements were made, in triplicate.

Equilibrium uptake of water as a function of relative humidity (RH) for crystalline and amorphous samples to define the equilibrium water sorption isotherms was measured at 25°C . The relative standard deviation associ-

ated with water sorption data was within $\pm 5\%$ of the reported value. Mass transfer equilibrium was insured by attaining a rate of mass change of less than $0.2 \mu\text{g}/\text{min}$ before increasing the humidity. Crystallinity was checked after each measurement, and with one exception (glipizide, where water loss was noted near the end of the isotherm), samples remained amorphous, and solute activity data were obtained as a function of water activity, were either linear or quadratic with slight curvature throughout the range of water activities (1), and were extrapolated slightly beyond the actual data to unity water activity to obtain the activity of solute in the solid at saturation. The glipizide data at relative humidities at which the solid exhibited a loss in water content as humidity increased were excluded from analysis as this phenomenon clearly indicated crystallization (Fig. 1).

Melting point (T_m) and heat of fusion (ΔH_f) of crystalline samples, glass transition temperature (T_g) and heat capacity change at T_g for amorphous materials, and heat capacity at constant pressure (C_p) for both crystalline and amorphous

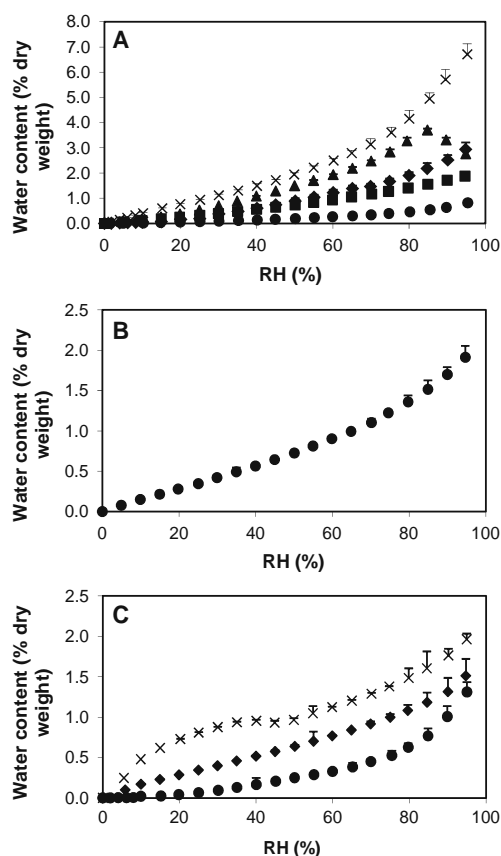


Fig. 1 Water sorption isotherms for amorphous solids at 25°C ($n = 3$) for Acids (**A**; \times hydrochlorothiazide, (black triangle) glipizide, (black diamond suit) indomethacin, (black square) glybenclamide, (black circle) iopanoic acid), Base (**B**; (black circle) terfenadine), and Non-ionizable (**C**; \times spironolactone, (black diamond) danazol, (black circle) griseofulvin).

samples were measured by differential scanning calorimetry (DSC) as previously described (1). The standard deviation associated with T_m was $\pm 0.3^\circ\text{C}$, $\pm 1.0^\circ\text{C}$ for T_g and $\pm 0.6\text{ J/g}$ for ΔH_f . The relative standard deviations associated with the heat capacity measurements were within $\pm 3\%$.

The ionization constant (pKa) of each ionizable drug was determined from the pH-solubility profile. The standard deviation associated with pKa values were within ± 0.2 units of the reported value, with the exception of glybenclamide. Due to its low solubility, it was difficult to obtain an unambiguous fit to the pH-solubility profile. The pKa reported in Table I is consistent with the pH-solubility profile obtained here as well as the pKa obtained by Manderscheid and Eichinger (21).

Determination of Experimental Solubility

Solubilities¹ of both crystalline and amorphous forms of the model compounds studied were measured in de-ionized water at 25°C . Solubility measurements were made in a USP type II (paddle) apparatus (Distek dissolution system 2100C, Distek Inc., North Brunswick, NJ). An excess of either crystalline or amorphous powdered drug was added to 250 mL of water. The aqueous solubilities of most crystalline compounds were less than $30\text{ }\mu\text{g/mL}$. Solubility experiments with amorphous drug were generally conducted using a suspension concentration of 2 mg/mL , which was approximately 50 times the solubility of the crystalline drug and thus ensured the presence of excess solid during the measurement of solubility. Presence of excess drug was also confirmed visually during the solubility measurement. In the case of hydrochlorothiazide, a suspension concentration of 10 mg/mL was used due to significantly higher solubility of the crystalline compound. The solubility measurements were conducted using a paddle speed of 300 rpm to disperse the powder in the dissolution vessel. Both crystalline and amorphous solids were screened through a 100-mesh screen ($150\text{ }\mu$ size opening) and retained on 200-mesh screen ($75\text{ }\mu$ size opening). This procedure was utilized specifically to overcome some experimental challenges of reproducibly measuring solubility of amorphous drugs, which are described in the next paragraph. Solubility measurements were carried out in triplicate for both crystalline and amorphous solutes.

Since most amorphous solutes were expected to undergo solvent-mediated transformation to a crystalline form upon

equilibration with water, the experimental assessment of their equilibrium solubility presented serious difficulties. Practical challenges involved in measuring peak concentration of amorphous solutes reproducibly included difficulty in wetting and dispersing the drug in aqueous medium in addition to the tendency to re-crystallize during the dissolution experiment. To overcome variability, the particle size was controlled so that peak concentrations were more reproducible. The peak concentration observed during dissolution of solute in the presence of excess solid was used as the estimate of solubility for an amorphous solute. However, for a system undergoing re-crystallization during dissolution, this estimate of solubility will always produce a result lower than the actual equilibrium solubility of the amorphous phase. The relative standard deviations of solubility values were within $\pm 2\%$ of reported value for crystalline drug and within $\pm 5\%$ of the reported value for amorphous drug. Note that precision does not necessarily indicate accuracy; due to re-crystallization during the measurement, the reported solubility of an amorphous form may be subject to serious systematic error and is an "apparent solubility" (22), determined as the maximum in concentration in the concentration-time curve found during dissolution of the solid.

To separate solid from solution, all solubility samples were filtered through a $0.22\text{ }\mu$ syringe filter (Acrodisc®, Gelman Sciences), and the first few milliliters of sample were discarded to minimize losses due to adsorption. The discard volume selected for each compound was based on a separate filter validation experiment. The solution samples from solubility studies were diluted appropriately with mobile phase solvent to prevent crystallization of solute and then analyzed by reverse-phase gradient HPLC to determine the drug concentration in solution. An apparent experimental solubility ratio $R_{S\text{ Expt}}$ was calculated from Eq. 2:

$$R_{S\text{ Expt}} = \frac{C_T^a}{C_T^x} \quad (2)$$

where C_T^a is the peak concentration of amorphous solute (or "apparent solubility"), and C_T^x is the equilibrium solubility of crystalline solute.

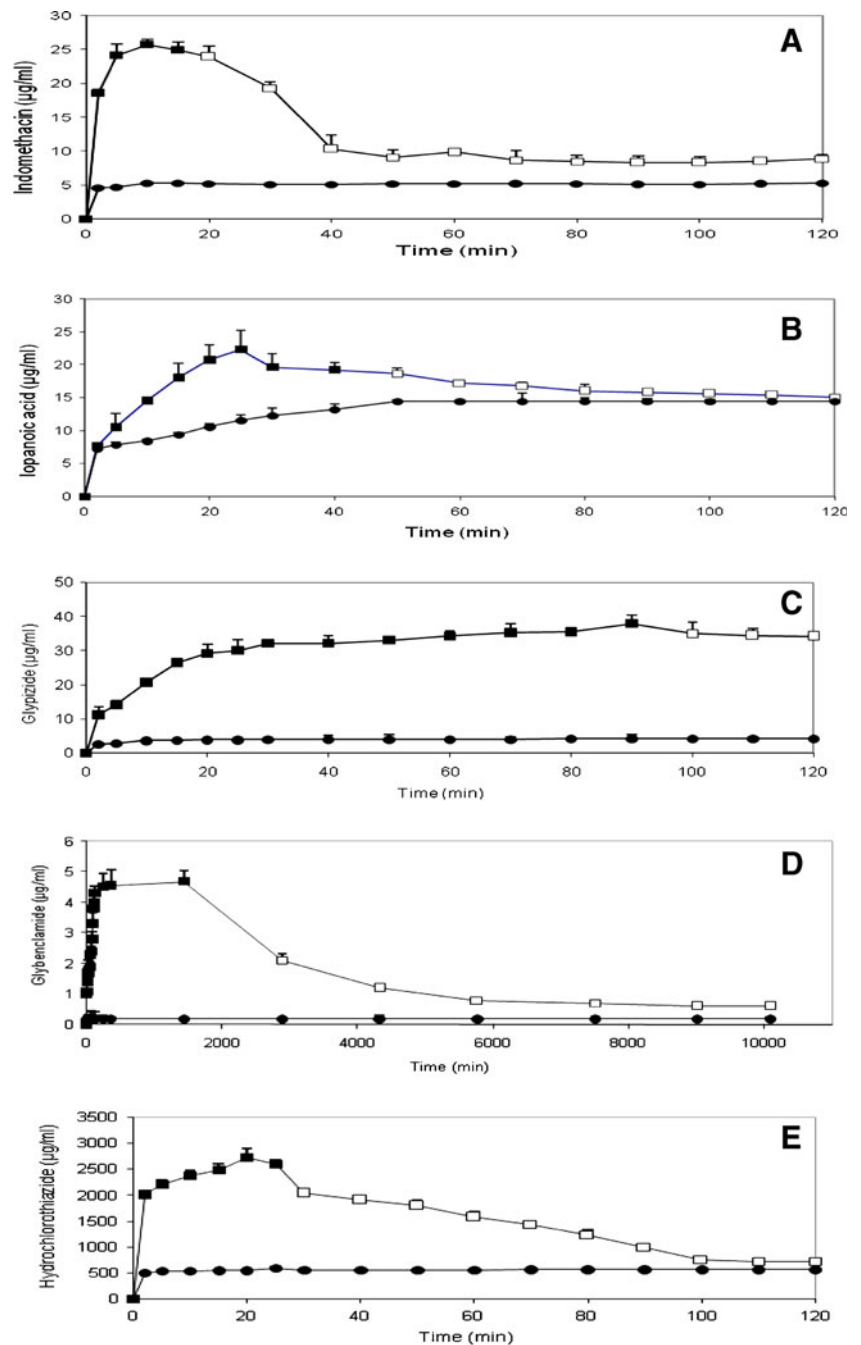
A portion of each sample taken at each time point during measurement of amorphous drug solubility was immediately (within 2 min) observed under the polarized light microscope for birefringence. The time points in Figs. 2, 3, 4 in which birefringence was observed are designated by open symbols.

HPLC Analysis

The concentrations of compounds used in the solubility studies were analyzed by reverse-phase gradient HPLC. A universal HPLC method was developed for the analysis of all

¹ The term *solubility*, when used in the context of an amorphous form, does not necessarily refer to the thermodynamic solubility and should be interpreted as an "apparent solubility," which may be significantly lower than the true thermodynamic value.

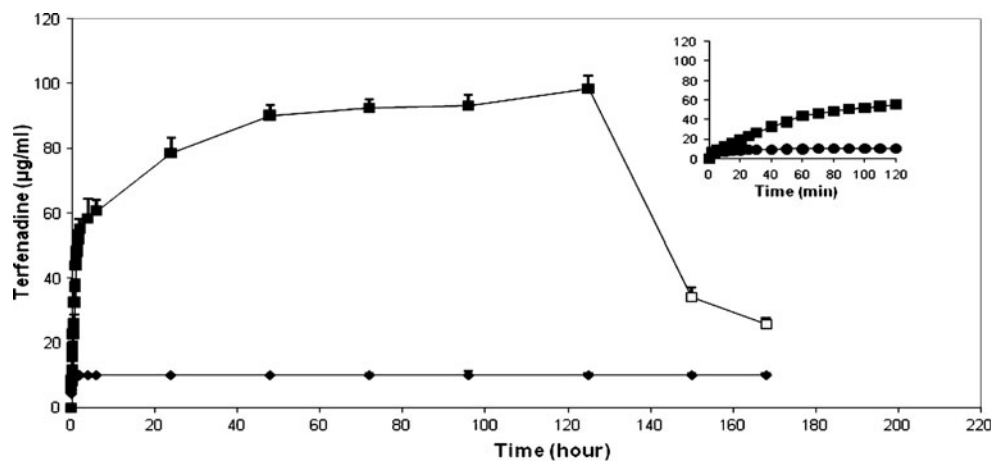
Fig. 2 Experimental concentration-time profiles during dissolution of acidic drugs ($\mu\text{g/ml}$). Indomethacin **A**, Iopanoic acid **B**, Glipizide **C**, Glybenclamide **D** and Hydrochlorothiazide **E** ((black circle) crystal; (black square) amorphous; (white square) presence of crystallinity in amorphous sample was observed at these time points).



nine drugs studied. The HPLC analyses were performed using an Agilent 1,100 serial system (Agilent Technologies, Palo Alto, CA) equipped with a 3.9 mm \times 150 mm C18 column (SymmetryShield, Waters, Milford, MA). The column temperature was 25°C, and the wavelength of detection was set to 210 nm. The mobile phase consisted of binary gradient of solvent A (acetonitrile) and solvent B (water with 0.1% trifluoroacetic acid). The linear gradient started at 5% A and increased to 95% A in 25 min, followed by a return to the starting condition within 2 min and equilibrated at the starting

condition for 3 min. The injection volume was 20 μL . The flow rate was 1.0 mL/min, and total run time was set for 30 min. This universal, reverse-phase gradient method provided baseline resolution and excellent peak characteristics for each model compound. Quantification of drug concentrations was performed by analysis of peak area using Agilent Chemstation® software. In each case, concentrations in the solubility samples were at least ten times higher than the limit of quantitation of the assay except for glybenclamide and danazol, where they were at least three-fold higher.

Fig. 3 Experimental concentration-time profiles during dissolution of basic drug ($\mu\text{g/ml}$). Terfenadine ((black circle) crystal; (black square) amorphous; (white square) presence of crystallinity in amorphous sample was observed at these time points).



RESULTS AND DISCUSSION

Thermal Properties and Ionization (pKa)

The molecular structures and properties of the diverse set of water-insoluble model compounds used in this study are

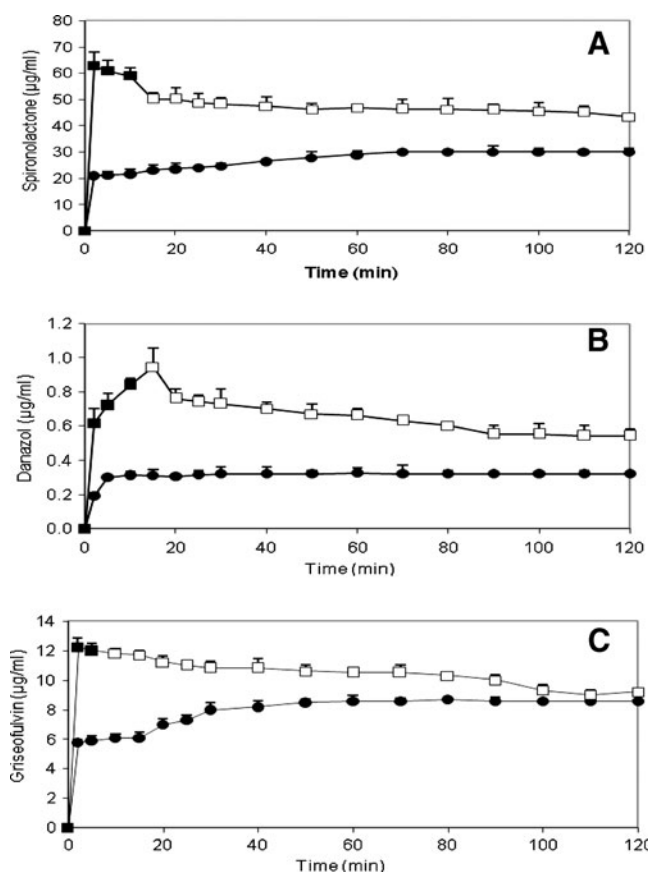


Fig. 4 Experimental concentration-time profiles during dissolution of non-ionizable drugs ($\mu\text{g/ml}$). Spirolactone **A**, Danazol **B**, and Griseofulvin **C** ((black circle) crystal; (black square) amorphous; (white square) presence of crystallinity in amorphous sample was observed at these time points).

given in Table I. Experimentally determined thermal properties for each of these model compounds are summarized in Table II. Thermal properties such as melting point (T_m) and heat of fusion (ΔH_f) were measured for crystalline solutes, whereas glass transition temperature (T_g) and heat capacity change at T_g ($\Delta C_{p,Tg}$) were measured for amorphous solutes.

The thermal properties for this limited set of model compounds represent a wide range of values. The melting points spanned a range of 116.2 K (423.2 to 539.4 K), and the glass transition temperatures varied over a range of 72 K (315.4 to 387.3 K). These large differences in T_m and T_g values for organic molecules (glasses) likely reflect differences in H-bond interactions in the solids (23,24). The heat of fusion values ranged from 30.0 to 55.4 KJ/mole, and the heat capacity difference between crystal and liquid ($\Delta C_{p,x,l}$) values ranged from 92 to 448 J/molK. The temperature of re-crystallization (T_c) of the amorphous solid, as measured during a DSC warming scan at 2 K/min with an oscillation period of 60 s and amplitude of ± 0.5 K on the amorphous solid, spanned a range of 77 K (376 to 453 K), which was similar to the range of values for T_g . At least for these compounds, the kinetic parameters, both T_g and T_c , are not directly related to their thermodynamic properties, such as T_m and ΔH_f . The difference between kinetic and thermodynamic properties of amorphous drugs is clearly exemplified by danazol and indomethacin. Although these two compounds have identical temperatures of re-crystallization, their glass transition temperatures differ by 30 K, and their melting points differ by 58 K. Similarly, it is generally not useful to use structural and thermal properties to predict kinetic properties, such as the maximum in concentration during dissolution when re-crystallization occurs.

The free energy difference between amorphous and crystal form ($\Delta \bar{G}_{x,a}^0(T)$) of the model compounds at 298 K are shown in Table II. These values were calculated

Table II Thermal Properties of Amorphous and Crystal Forms of Acid, Base and Non-Ionizable Compounds

Drug	T_m (°K)	T_g (°K)	T_c (°K)	ΔH_f (kJ/mol)	ΔC_{pTg} (J/molK)	$\Delta C_{p^{x,l}}$ (J/molK)	$\Delta G_{x,d}^0(298)$ (kJ/mol)
Indomethacin	435.2	317.6	376.4	36.5	132.4	164.6	8.4
Iopanoic acid	425.6	315.4	379.2	30.0	87.9	154.1	6.3
Glipizide	471.5	331.3	382.0	55.4	365.3	447.9	9.7
Glybenclamide	446.9	321.6	403.1	55.4	197.1	296.4	12.1
Hydrochlorothiazide	539.4	387.3	453.4	37.6	113.1	178.6	10.5
Terfenadine	423.2	332.6	399.3	42.4	254.7	292.4	9.4
Griseofulvin	494.2	363.6	393.9	37.8	102.3	204.6	8.6
Spironolactone	480.4	353.6	402.3	41.0	50.0	91.7	13.1
Danazol	492.8	348.0	376.2	31.9	60.7	118.1	8.8

T_m , melting temperature; T_g , glass transition temperature; T_c , crystallization temperature; ΔH_f , heat of fusion; ΔC_{pTg} , heat capacity at glass transition; $\Delta C_{p^{x,l}}$, heat capacity (crystal-liquid); $\Delta G_{x,d}^0(298)$, free energy difference between amorphous and crystal form of drug at 298 K calculated from Eq. 1 in reference (1)

utilizing thermal data on crystal (T_m and ΔH_f) and amorphous forms (T_g and ΔC_{pTg}) as well as the heat capacity difference between crystal and liquid ($\Delta C_{p^{x,l}}$), utilizing Eq. 1 as described in the previous report (1).

The ionization constant (pKa) values for acids and bases determined using the pH solubility profile are shown in Table I, as are the experimentally measured pKa values were used for indomethacin (25), iopanoic acid (26), terfenadine (27), and glipizide (28). For glybenclamide, due to poor aqueous solubility, literature pKa value was used (21).

Moisture Sorption and Solute Activity

The water sorption isotherms for the amorphous forms of model compounds at 25°C are shown in Fig. 1a, b and c for acids, bases, and non-ionizable compounds, respectively. The number of moles of water absorbed per mole of solid solute was measured gravimetrically up to 95% RH. Solute activity was calculated by numerical integration of the Gibbs-Duhem equation using moisture sorption isotherm data collected up to 95%RH (i.e. water activity=0.95) (1). The calculated activity of the solute was then extrapolated to 100%RH (i.e. water activity=1) from a plot of solute activity vs. water activity. During the course of these moisture sorption experiments, only glipizide was observed to partially crystallize on the moisture sorption balance above 85% RH, thereby losing some of the absorbed water during partial transformation to the crystalline form. The water uptake for the amorphous compounds studied ranged from 1 to 7 wt% at the maximal RH of 95%. Among compounds with acidic functionality, hydrochlorothiazide is most polar (i.e. lowest logP) and, as expected, was found to absorb higher amounts of water. Although for the six ionizable compounds there seems to be an inverse relationship between logP and equilibrium moisture uptake at 95% RH, no such trend is obvious for the neutral compounds (Fig. 1c).

Experimental Apparent Solubilities

The experimentally determined concentration-time profiles for the amorphous and crystalline forms of acidic, basic, and non-ionizable compounds are shown in Figs. 2, 3 and 4, respectively. The time points at which crystals were observable by polarized light microscopy in the initially amorphous suspensions are represented by open symbols in Figs. 2, 3 and 4. Amorphous forms of all the model compounds studied consistently achieved significantly higher concentrations in water than their crystalline forms, at least during the first 30 min of apparent solubility measurements at 25°C. The time, rate, and extent of re-crystallization of the amorphous form during contact with water were unique to each compound. The observed characteristics of the concentration-time profiles could not be correlated to either structure or physico-chemical properties of compounds.

The approximate times required for amorphous samples to at least partially crystallize during the apparent solubility determination, as detected by the first appearance of crystals under polarized light microscopy, are summarized in Table III. The amorphous forms of the basic compound (terfenadine) tended to dissolve slowly, as it did not disperse well and seemed to resist wetting, and the powder tended to agglomerate. Terfenadine required up to 7 days at room temperature to partially convert to its crystalline form.

The experimental solubility enhancement ratios, $R_{S, \text{Expt}}$, calculated using the peak concentration for the amorphous apparent solubility, are compared with the theoretically calculated ratio for all compounds in Table IV. In all cases, the experimental enhancement ratio was less than the theoretical, as expected, due to solvent-mediated crystallization (with the exception of glybenclamide). The data in Table IV show the importance of each of the three factors from Eq. 1 in achieving an accurate prediction. For

Table III Comparison of Proposed Indicators of Re-crystallization Tendency with the Differences in Solubility Enhancement Ratio (Theory vs. Expt.) and Visually Observed Crystallization Onset in Solution

Drug	Crystallization onset time ^a (min)	$\frac{R_S^{\text{Theory}}}{R_S^{\text{Expt.}}} = \text{Fold difference in prediction}$	$\frac{T_c - T_g}{T_m - T_g}$ ^c
Indomethacin	20	1.4	0.50
Iopanoic acid	50	3.8	0.58
Glipizide	100	1.2	0.36
Glybenclamide	2880	0.8 ^b	0.65
Hydrochlorothiazide	25	6.8	0.43
Terfenadine	9000	1.3	0.74
Griseofulvin	10	21	0.23
Spirolactone	15	53	0.38
Danazol	15	8.8	0.19

^a Time-point of first detectable crystals observed during experimental solubility determination of amorphous drug (visual observation under polarized light microscope); ^b Ionization of glybenclamide is extensive (90%) hence theoretical solubility enhancement calculations are quite sensitive to experimental errors in pKa measurement. For example ± 0.3 units error in measurement of glybenclamide pKa (5.5) would cause variation in the "fold difference" prediction from 0.51 to 1.1 (mean value 0.8); ^c reduced temperature (ref. Zhou et al. (31))

example, in the case of glipizide, the theoretically estimated solubility ratio is 11.1 when all three contributing factors are considered. When the impacts of ionization and water sorption were neglected, the ratios were 23.8 and 23.5, respectively. Thus, both ionization and water sorption significantly impact the solubility enhancement ratio, reducing the value that would be calculated if one were only to consider the free energy difference between the crystal and neat glass. Even for non-ionizable compounds, water sorption had a significant impact on theoretically estimated solubility ratio. For example, in the case of

hydrochlorothiazide (negligible ionization), reduction in solute activity due to water sorption reduced the ratio from 69.1 to 33.9. Therefore, the analysis by factor in Table IV clearly demonstrates that all three factors, ionization, water sorption, and free energy difference between forms, must be considered to get an accurate estimate of solubility enhancement ratio for amorphous drug according to Eq. 1.

The experimental and theoretical predictions of solubility enhancement ratios are quantitatively compared in Table IV. We observed a 0.8- to 53-fold difference between theoretical and experimental solubility enhancement ratios

Table IV Comparison of Theoretical and Experimental Solubility Enhancement Ratios (Amorphous/Crystal) and Contribution of the Three Factors in Eq. 1 to the Enhancement Ratio

Drug	Experimentally Determined Solubility Enhancement Ratio ($R_S^{\text{Expt.}}$)	Theoretically Estimated Solubility Enhancement Ratio (R_S^{Theory})			
		Contributing Factors Considered			
		ionization, water sorption and Gibbs free energy (1)	Gibbs free energy only (2)	Water sorption and Gibbs free energy only (3)	Gibbs free energy and ionization only (4)
Indomethacin ^a	4.9	7.0	29.0	20.8	9.9
Iopanoic acid	1.5	5.7	12.5	10.9	6.5
Glipizide	9.2	11.1	50.6	23.8	23.5
Glybenclamide	22.6	17.1	130.6	86.3	25.9
Hydrochlorothiazide	4.9	33.9 ^b	69.1	33.9	69.1 ^b
Terfenadine	10	13.0	43.6	29.0	19.4
Griseofulvin	1.4	29.1 ^b	32.1	29.1	32.1 ^b
Spirolactone	2.1	110.3 ^b	195.9	110.3	195.9 ^b
Danazol	3.0	26.5 ^b	34.4	26.5	34.4 ^b

^a data reported in ref. (1); ^b ionization factor is unity for non-ionizable compounds and hydrochlorothiazide which has negligible ionization in water; (1) theoretical solubility enhancement ratio calculated using all three factors, ionization, water sorption and Gibbs free energy in Eq. 1 at 25°C; (2) theoretical solubility enhancement ratio calculated using Gibbs free energy only; (3) theoretical solubility enhancement ratio calculated using Gibbs free energy and water sorption only; (4) theoretical solubility enhancement ratio calculated using Gibbs free energy and ionization only in Eq. 1

(Table III). The differences between theory and experiment for spiranolactone, griseofulvin and danazol, three of the non-ionizable compounds, were found to be 53-, 21- and 8.8- fold, respectively. These were the largest differences among all compounds studied and are a direct consequence of the rapid re-crystallization during the experiment. Based on the polarized light microscopy (PLM) results, amorphous spiranolactone, danazol and griseofulvin were found to crystallize within 15 to 20 min of coming in contact with water during solubility measurements (Fig. 4a, b and c). The rapid crystallization of amorphous griseofulvin in water is in direct contrast to the reported slow rate in the dry amorphous state, even when heated to temperatures above T_g (29). This contrast in re-crystallization tendency might reflect greatly enhanced molecular mobility of amorphous griseofulvin when it is hydrated; alternatively, the re-crystallization may be related to the ability of the supersaturated solution above the dissolving solid to nucleate and crystallize on the surface of the amorphous particles (30). It is not possible to differentiate between solution-mediated nucleation and nucleation in the hydrated amorphous solid in the current study. However, regardless of the mechanism, rapid re-crystallization is clearly a critical factor in determining the concentration-time curve, so compounds were classified as rapid or slow crystallizers in solution during the apparent solubility measurements, based on the observations made with PLM. Both danazol and griseofulvin were found to be rapid crystallizers in solution, reducing the experimental solubility enhancement from the theoretical prediction. In both cases, crystals were observed during dissolution of amorphous solid within 15 min.

For glipizide, terfenadine and indomethacin, there was good agreement between the theoretically estimated apparent solubility ratios and experimental measurements. This agreement can be attributed to the low propensity for crystallization of these compounds during the earliest time points of solubility measurement, thus enabling attainment of the theoretical solubility of the amorphous form prior to crystallization. Crystals of glipizide were observed in the amorphous samples at 100 min (Fig. 2c), whereas no crystals were observed in the case of terfenadine up to 150 h (about 1 week, Fig. 3) and with glybenclamide for up to 48 h (Fig. 2d). Indomethacin had a relatively fast crystallization time but still showed reasonably good agreement between experimental and theoretical solubility enhancements. Crystallization time was monitored by birefringence under cross polarizers, which cannot readily distinguish which polymorph is appearing. Recently, an unidentified polymorph of indomethacin was seen during dissolution of amorphous indomethacin (30). The solubility of that polymorph may be high and may contribute to the ability of indomethacin to sustain its high concentration.

Additionally, iopanoic acid and hydrochlorothiazide were intermediate crystallizers when suspended in water (Fig. 2b and e), and there was fair agreement between theoretically estimated and experimentally measured solubility ratio for both iopanoic acid and hydrochlorothiazide (3.8- and 6.8-fold difference in apparent solubility enhancement ratio). The fast crystallizers, danazol, griseofulvin and spiranolactone had experimental solubilities that were much lower than predicted. For glybenclamide, the ratio of theoretical to experimental solubility was slightly less than unity (0.8-fold difference in apparent solubility enhancement ratio, Table III), which was likely due to “normal” experimental error in pKa coupled with its extensive ionization in solution, thereby making the prediction highly sensitive to even small errors in dissociation constant (pKa).

Given the difficulties created by re-crystallization during an attempt to determine solubility, it was recognized that it would be beneficial to the formulator to identify compounds that may have lower propensity toward crystallization when amorphous drug comes in contact with water. Zhou *et al.* (31) have suggested a reduced crystallization temperature $\left(\frac{T_c - T_g}{T_m - T_g}\right)$ for comparing the ease of crystallization of compounds from the neat amorphous dry state. In their work, a low reduced temperature correlated with faster re-crystallization in the amorphous solid. Table III summarizes the reduced temperature values calculated using the Zhou relationship for the model compounds studied in the present research. The Zhou scheme also suggests that danazol and griseofulvin should be fast crystallizers in solution.

SUMMARY AND CONCLUSIONS

A detailed thermodynamic approach developed previously (1) to estimate the enhancement in solubility that can be achieved with the amorphous form of a drug was shown to be consistent with experimental apparent solubility data for eight other structurally diverse compounds. These model water-insoluble compounds represented both different ionization states (acid, base and non-ionizable) and diverse other molecular properties (melting point and octanol-water partition coefficient). Results from these investigations confirmed that all three factors, degree of ionization (when applicable), free energy difference between pure crystalline and pure amorphous forms, and solute activity reduction by moisture sorption, contribute to varying degrees to the solubility advantage of amorphous pharmaceuticals. The magnitude of the impact of each of these factors, (i.e. degree of ionization, free energy difference via DSC data, and moisture sorption) is dependent on physicochemical properties of the molecule. The equation and methodology for calculating solubility enhancement is a

significant improvement over the previously reported (9) method, because the degree of ionization and the moisture sorption effects significantly decrease the theoretical solubility enhancement of the amorphous form.

The theoretical solubility enhancement ratios are in close agreement with the experimental solubility ratios calculated using apparent solubilities of the amorphous solid under conditions where crystallization during the apparent solubility determination is slow. Conversely, when crystallization of the amorphous solid occurs rapidly during the solubility measurement, the theoretically estimated solubility enhancement ratio is much greater than the experimental ratio. The reduced temperature previously reported (31) was also used to predict the propensity of solvent-mediated re-crystallization of amorphous solids and provides a rough prediction for the formulator interested in advancing the amorphous form of a drug in the development process. The thermodynamic approach for calculation of solubility enhancement via the amorphous phase provides a convenient and accurate estimate of the maximum enhancement possible for an amorphous form of a drug. We suggest that this procedure for assessment of solubility advantage of the amorphous form would be valuable in guiding a decision on selection of methodology for bioavailability enhancement of an insoluble compound.

REFERENCES

- Murdande SB, Pikal MJ, Shanker RM, Bogner RH. Solubility advantage of amorphous pharmaceuticals: I. A thermodynamic analysis. *J Pharm Sci*. 2010;99:1254–64.
- Hancock BC, Zografi G. Characteristics and significance of the amorphous state in pharmaceutical systems. *J Pharm Sci*. 1997;86:1–12.
- Yu L. Amorphous pharmaceutical solids: preparation, characterization and stabilization. *Adv Drug Deliv Rev*. 2001;48:27–42.
- Craig DQ, Royall PG, Kett VL, Hopton ML. The relevance of the amorphous state to pharmaceutical dosage forms: glassy drugs and freeze dried systems. *Int J Pharm*. 1999;179:179–207.
- Kaushal AM, Gupta P, Bansal AK. Amorphous drug delivery systems: molecular aspects, design and performance. *Crit Rev Ther Drug Carr Syst*. 2004;21:133–93.
- Li DX, Oh Y-K, Lim S-J, Kim JO, Yang HJ, Sung JH, *et al*. Novel gelatin microcapsule with bioavailability enhancement of ibuprofen using spray-drying technique. *Int J Pharm*. 2008;355:277–84.
- Kim J-S, Kim M-S, Park HJ, Jin S-J, Lee S, Hwang S-J. Physicochemical properties and oral bioavailability of amorphous atorvastatin hemi-calcium using spray-drying and SAS process. *Int J Pharm*. 2008;359:211–9.
- Vasconcelos T, Sarmiento B, Costa P. Solid dispersions as strategy to improve oral bioavailability of poor water soluble drugs. *Drug Discov Today*. 2007;12:1068–75.
- Hancock BC, Parks M. What is the true solubility advantage for amorphous pharmaceuticals? *Pharm Res*. 2000;17:397–404.
- Chawla G, Gupta P, Thilagavathi R, Chakraborti AK, Bansal AK. Characterization of solid-state forms of celecoxib. *Eur J Pharm Sci*. 2003;20:305–17.
- Bansal SS, Kaushal AM, Bansal AK. Molecular and thermodynamic aspects of solubility advantage from solid dispersions. *Mol Pharmaceutics*. 2007;4:794–802.
- Ran Y, Neera J, Yalkowsky SH. Solubility and partitioning of aqueous solubility of organic compounds by the General Solubility Equation (GSE). *J Chem Inf Comput Sci*. 1980;41:1208–17.
- Yalkowski SH, Valvani SC. Solubility and partitioning I: solubility of nonelectrolytes in water. *J Pharm Sci*. 1980;69:912–22.
- Neera J, Yalkowsky SH. Estimation of the aqueous solubility I: application to organic nonelectrolytes. *J Pharm Sci*. 2001;90:234–52.
- Yalkowsky SH. Estimation of the aqueous solubility of complex organic compounds. *Chemosphere*. 1993;26:1239–61.
- Yalkowsky SH. Solubility and partitioning V: dependence of solubility on melting point. *J Pharm Sci*. 1981;70:971–3.
- Amidon GL, Williams NA. A solubility equation for nonelectrolytes in water. *Int J Pharm*. 1982;11:249–56.
- <http://www.who.int/medicines/publications/essentialmedicines/en/>. WHO Model List. Essential Medicines. <http://www.who.int/medicines/publications/essentialmedicines/en/>.
- Lipinski CA, Lombardo F, Dominy BW, Feeney PJ. Experimental and computational approaches to estimate solubility and permeability in drug discovery and development settings. *Adv Drug Deliv Rev*. 1997;23:3–25.
- Lipinski CA, Lombardo F, Dominy BW, Feeney PJ. Experimental and computational approaches to estimate solubility and permeability in drug discovery and development settings. *Adv Drug Deliv Rev*. 2001;46:3–26.
- Manderschid M, Eichinger T. Determination of pKa values by liquid chromatography. *J Chromatogr Sci*. 2003;41:323–6.
- Murdande SB, Pikal M, Shanker R, Bogner R. Aqueous solubility of crystalline and amorphous drugs: challenges in measurement. *Pharm Dev Technol*. (2010). doi:10.3109/10837451003774377.
- Johari GP, Shanker RM. Calorimetric relaxation and the glass-liquid temperature range of acetaminophen-nifedipine alloys. *J Pharm Sci*. 2007;9999:n/a .
- Tombari E, Presto S, Johari G, Shanker R. Molecular mobility, thermodynamics and stability of Griseofulvin's ultraviscous and glassy states from dynamic heat capacity. *Pharm Res*. 2008;25:902–12.
- Wan H, Holmen AG, Wang Y, Lindberg W, Englund M, Nagard MB, *et al*. High-throughput screening of pKa values of pharmaceuticals by pressure-assisted capillary electrophoresis and mass spectrometry. *Rapid Commun Mass Spectrom*. 2003;17:2639–48.
- Gerakis AM, Koupparis MA, Efstathiou CE. Micellar acid–base potentiometric titrations of weak acidic and/or insoluble drugs. *J Pharm Biomed Anal*. 1993;11:33–41.
- Chiang P-C, Foster KA, Whittle MC, Su C-C, Pretzer DK. Medium throughput pKa determinations of drugs and chemicals by reverse phase HPLC with an organic gradient. *J Liq Chromatogr Relat Technol*. 2006;29:2291–301.
- Wiczling P, Kawczak P, Nasal A, Kalisz R. Simultaneous determination of pKa and lipophilicity by gradient RP HPLC. *Anal Chem*. 2006;78:239–49.
- Zhou D, Zhang GGZ, Law D, Grant DJW, Schmitt EA. Thermodynamics, molecular mobility and crystallization kinetics of amorphous griseofulvin. *Mol Pharm*. 2008;5:927–36.
- Greco K, Bogner RH. Crystallization of amorphous indomethacin during dissolution: Effect of processing and annealing. *Mol Pharm* (2010). doi:10.1021/mp1000197.
- Zhou D, Zhang GGZ, Law D, Grant DJW, Schmitt EA. Physical stability of amorphous pharmaceuticals: Importance of configurational thermodynamic quantities and molecular mobility. *J Pharm Sci*. 2002;91:1863–72.